Texture Analysis of the Liver at MDCT for Assessing Hepatic Fibrosis

Original Research

Abstract:

Purpose: To evaluate CT texture analysis (CTTA) for staging of hepatic fibrosis (stages F0-F4)

Methods: Quantitative texture analysis (QTA) of the liver was performed on abdominal MDCT scans using commercially-available software (TexRAD), which uses a filtration histogram statistic-based technique. Single-slice ROI measurements of the total liver, Couinaud segments IV-VIII, and segments I-III were obtained. CTTA parameters were correlated against fibrosis stage (F0-F4), with biopsy performed within one year for all cases with intermediate fibrosis (F1-F3).

Results: The study cohort consisted of 289 adults (158M/131W; mean age, 51 yrs), including healthy controls (F0, n=77), and patients with increasing stages of fibrosis (F1, n=42; F2 n=37; F3 n=53; F4 n=80). Mean of the pixel histogram increased with fibrosis stage, demonstrating an ROC AUC of 0.78 at medium filtration for F0 vs F1-4, with sensitivity and specificity of 74% and 74% at cut-off 0.18. For significant fibrosis (≥F2), mean showed AUCs ranging from 0.71-0.73 across medium and coarse filtered textures with sensitivity and specificity of 71% and 68% at cutoff of 0.3, with similar performance also observed for advanced fibrosis (≥F3). Entropy showed a similar trend. Conversely, kurtosis and skewness decreased with increasing fibrosis, particularly in cirrhotic patients. For cirrhosis (≥F4), kurtosis and skewness showed AUCs of 0.86 and 0.87 respectively at coarse filtered scale, with skewness showing a sensitivity and specificity of 84% and 75% at cutoff of 1.3.

Conclusion: CTTA may be helpful in detecting the presence of hepatic fibrosis and discriminating between stages of fibrosis, particularly at advanced levels.

Key words: CT Texture analysis, Hepatic fibrosis, liver disease, cirrhosis

Introduction:

Chronic liver disease has many potential etiologies, ranging from viral infection to non-alcoholic fatty liver disease, some of which are on the rise, with an estimated 30 million Americans affected [1, 2]. The end stage of liver disease is fibrosis and eventual cirrhosis. Assessment of fibrosis is important for diagnosis, but also increasingly for management decisions and follow up, particularly in evaluating candidacy for and response to novel and emerging therapies. Although liver biopsy has been the reference standard in the diagnosis and staging of fibrosis, it has disadvantages in that it is an invasive technique with relatively high cost and potential sampling error [3, 4]. Non-invasive imaging techniques for staging hepatic fibrosis have shown great promise and increased adoption, with the most attention given to elastography techniques. There is a growing body of data showing that MR and US elastography are safe, non-invasive and reliable techniques for evaluating fibrosis [1, 5-12]. However, these techniques must be performed prospectively with dedicated equipment, may be influenced by operator/technical and patient factors, and rely on measurement of tissue stiffness. Diseases other than fibrosis, such as inflammation, biliary obstruction, and congestion, can also increase liver stiffness [1].

There is an ongoing clinical need for robust non-invasive imaging biomarkers to detect and stage hepatic fibrosis. A variety of morphologic and volumetric changes in the liver and spleen have been evaluated on CT, recently including the liver segmental volume ratio (LSVR), splenic volume, and liver surface nodularity [13-16]. These measurements can be performed retrospectively without special equipment and have preliminarily shown performance similar to elastography techniques. CT texture analysis is an emerging technique that quantifies heterogeneity of a region of interest by analyzing the distribution and/or relationship of pixel or voxel gray levels in the image [17]. This technique has been most intensely studied in oncologic applications, and has shown association with pathologic features and clinical outcomes in a variety of tumor types [18-31]. Some non-oncologic applications are being evaluated, with several groups using texture analysis to assess emphysema and fibrosis in the lung [32, 33]. One small series using CT texture analysis to evaluate hepatic fibrosis found that texture parameters showed some ability to discriminate between stages of fibrosis, but the results were not very convincing [34]. Like volumetric assessment and surface nodularity, this technique can be easily retrospectively applied to CT images. Since it is assessing heterogeneity in the liver rather than tissue stiffness or macroscopic liver morphology, it has the potential to be complementary to other

techniques. The purpose of this study was to further evaluate CTTA for staging of hepatic fibrosis (stages F0-F4).

Methods:

This retrospective study was HIPAA compliant and IRB approved. The requirement for signed informed consent was waived.

Patient Population:

The final cohort consisted of 289 adult patients (158 M, 131 F, mean age 51 yrs). Patients were categorized based on stage of hepatic fibrosis (METAVIR stages F0-F4)[35] , ranging from normal controls (F0, n=77) through intermediate stages of fibrosis (F1, n=42; F2, n=37; F3, n=53) to end stage cirrhosis (F4, n=80). Inclusion criteria included adult patients, with both a liver biopsy and CT performed within 1 year for intermediate stages of fibrosis (F1-F3). Normal patients were asymptomatic healthy patients being evaluated for kidney donation and did not have a biopsy. The F4 group was defined by either a liver biopsy (n=36) or clear-cut chronic end-stage liver disease, as established by imaging and electronic medical review by an experienced abdominal radiologist. The latter definition required clear cross-sectional imaging evidence of cirrhosis and portal hypertension, identifiable clinical cause/risk factors for liver disease, and complication of liver disease (hepatic encephalopathy, variceal bleed). A portion of this cohort participated in separate investigations of hepatosplenic volume changes and surface nodularity [14-16]. In the majority of cases, the cause of underlying liver disease was hepatitis C, alcohol related liver disease, or non-alcoholic fatty liver disease, although small numbers of cases had other causes (primary sclerosing cholangitis, primary biliary cirrhosis, alpha 1 antitrypsin disease, cryptogenic).

MDCT technique:

All CT scans were obtained on 16- or 64-MDCT scanners. The specific CT protocol varied slightly based on the indication (i.e., triphasic liver for transplant evaluation, biphasic liver for cirrhotic liver evaluation, multiphasic exam for renal donor evaluation). For the CTTA measurement, portal venous phase images were used from all of the exams, using patient size based scan parameters (auto-mA, kV 100-140). Portal venous phase images were generally reconstructed with 5 mm slice thickness at 3 mm intervals at a matrix of 512 x 512 x 16.

CT Texture Analysis (CTTA):

CTTA was performed by a single trained reader under the supervision of two experienced abdominal radiologists (12 yrs, 22 yrs). Representative single-slice images at the level of the porta hepatis (largest cross section of the liver) were then sent to a commercially-available texture analysis research software platform (TexRAD Ltd, part of Feedback Plc, Cambridge, UK). Using the software, a region of interest (ROI) was manually drawn on a single slice at the level of the porta hepatis to include the entire liver (but exclude the major vessels) for a total liver measurement (Figure 1). A second ROI was drawn around the left lateral lobe and caudate (Couinaud segments I-III) with a third drawn around the medial left lobe and right lobe (Couinaud segments IV-VIII). This additional evaluation of segments I-III versus IV-VIII was based on the morphologic changes seen in cirrhosis and prior work looking at the liver segmental volume ratio (LSVR) [15, 16]. Previous studies have demonstrated that CTTA from a single-slice analysis have demonstrated the ability to extract sufficient information related to answer the clinical question and may not require multi-slice or volume analysis which have not shown to add significant benefit to the clinical application being researched (22, 36). Furthermore single-slice analysis reduces the computational time (is more practical in a routine radiological workflow) and complexities associated with multi-slice/volumetric analysis related to operator variability associated with ROI drawing particularly if the ROI drawing process involves manual/semi-automated segmentation approaches. CTTA technique employed in this study uses a filtration-histogram technique where initial filtration step using Laplacian of Gaussian (LoG) spatial band-pass (non-orthogonal Wavelet) filter to selectively extract and enhance features of different sizes and intensity variation [19, 30]. This produces a series of derived images that show features ranging from fine (spatial scaling factor, SSF 2 mm which corresponds to object size of 2 mm in radius), medium (SSF 3,4,5 mm which corresponds to object size of 3,4,5 mm in radius) to coarse (SSF 6, which corresponds to object size of approximately 6 mm in radius) texture maps (Figure 1) [36, 37]. This is followed by quantification using histogram-based statistical parameters (first, second and higher order) which includes mean gray level intensity (Mean), standard deviation (SD, dispersion from the mean), entropy (irregularity), mean of the positive pixels (MPP), skewness (asymmetry), and kurtosis (peakedness or sharpness) at each SSF value. Also, these histogram parameters were quantified from the conventional image without filtration (SSF=0) as a control. These values were recorded for each patient case and subsequently underwent statistical analysis. Texture features were correlated with stage of hepatic fibrosis.

Statistical analysis:

Examination of boxplots and Spearman rank correlates was used as a data reduction step to select features most highly correlated with fibrosis. This was seen in conjunction with a trend in significant correlation between a texture parameter vs fibrosis across the different SSF values (e.g. fine, medium, coarse) indicated a robust association, which would not be attributed to a chance correlation. A Mann-Whitney non-parametric U test was used to assess differences in the texture parameters selected from the data reduction step among the discrete F0-F4 cohorts with emphasis placed on the clinically relevant distinctions/groupings of presence of fibrosis (F0 vs F1-F4), significant fibrosis (≥F2), advanced hepatic fibrosis (≥F3) and cirrhosis (F4). ROC curves were obtained for each significant candidate metric from the Mann Whitney test, and AUC was calculated with DeLong 95% CI. Exploratory cutoffs for fibrosis categories were derived from the ROC analysis. A value of $p<0.05$ (two-sided) was the criterion for statistical significance. All statistical analyses were performed with the R program (version 3.3.1, R Core Team, 2016).

Results:

Mean gray level intensity (Mean) showed a statistically significant association with stage of fibrosis at nearly every SSF value (fine, medium and coarse texture scale) and for nearly all categorizations of fibrosis. Mean was seen to increase from F0 to F4 in the total liver measurement, and even more strongly in the segment IV-VIII measurement, particularly at medium (SSF 5 $p<0.001$) and coarse feature size (SSF 6, $p<0.001$). This association was seen less strongly (or possibly moving in the opposite direction) in segments I-III (Table 1, fig 2). ROC analysis of mean demonstrated an AUC of 0.78 at fine (SSF 2), 0.76 at medium (SSF 5, $p<0.001$) and 0.76 at coarse (SSF 6 $p<0.001$) feature size for differentiating F0 vs F1-4 (presence of any fibrosis, $p<0.001$, Table 2). A threshold of Mean >0.175 demonstrated a sensitivity and specificity of 74% and 74%, respectively (table 2). Mean demonstrated an AUC of 0.73 (medium texture scale, SSF 5) for identifying significant fibrosis (≥F2) and AUC of 0.73 for advanced fibrosis (≥F3; coarse texture scale, SSF 6). Mean demonstrated an AUC of 0.76 (coarse texture scale, SSF 6) for identification of cirrhosis (F4) with threshold of mean >0.94 with both sensitivity and specificity at 70% (Table 2, fig 3). Entropy and SD also showed some promise in identifying the presence of fibrosis with lower entropy and SD values in the F0 group compared to F1-F4, particularly at fine (SSF 2) filter levels, but at medium and coarse texture size filters for entropy as well. Again, this was seen in the total liver, but more prominently in segments IV-VIII.

Skewness and kurtosis of the pixel histogram also demonstrated association with hepatic fibrosis, which was particularly strong at identifying cirrhosis (F4). Skewness values were higher in the F4 group compared to the earlier stages of fibrosis, with a similar trend seen with kurtosis. This was seen at all filter levels (fine, medium and coarse texture scale) for kurtosis and mainly at medium (SSF 5) and coarse (SSF 6) texture scales for skewness. This was again seen in the total liver, but more prominently in segments IV-VIII for both measures, and to a lesser extent (or perhaps opposite direction for kurtosis) in segments I-III (Table 1, fig 4). For skewness at coarse filter (SSF 6), an AUC of 0.87 (95% CI 0.827, 0.919) was seen (F0-3 vs F4), with a threshold of <1.3 demonstrating sensitivity of 84% and specificity of 75%. Similarly, for kurtosis at coarse filter (SSF 6), an AUC of 0.86 (95 % CI 0.806, 0.909) was seen, with threshold < 5.2 showing sensitivity and specificity of 81% and 76% respectively (Table 2, fig 5).

Discussion:

We found that changes in liver parenchymal CT texture features are associated with degree of underlying hepatic fibrosis. As many of these patients undergo CT for other reasons, this is a measurement that can easily be performed retrospectively on routinely acquired scans without special equipment or complex technique. This may be helpful in both patients with known liver disease undergoing serial monitoring, but also for patients with unsuspected liver disease that is incidentally detected or first suggested on CT imaging. As improved therapies become available, the ability to detect and characterize fibrosis in at risk populations or monitor response to therapy in a non-invasive, global way becomes increasingly desirable. Techniques like CTTA would not necessarily eliminate the need for biopsy but minimize the frequency/streamline its usage as a method to triage need for biopsy or act as an adjunct to biopsy in discordant or complex cases.

Daginawala et al [34] looked at the use of texture analysis in assessing hepatic fibrosis in a cohort of 83 patients stratified by Ishak fibrosis scale and found that mean of the pixel histogram was a useful parameter, but with AUC of 0.68 for Ishak 0-2 vs 3-6, AUC of 0.68 for Ishak 0-3 vs 4-6 and 0.69 for Ishak 0-4 vs 5-6. They also saw some association with entropy [34]. We saw similar texture features (mean, entropy) associated with stage of fibrosis, but with more robust AUC values of approximately 0.75 in most cases (in the fair range of ROC curves), and with skewness and kurtosis showing ROC AUC values of 0.86-0.87 (good accuracy, near excellent). It is not clear that a filtration step was used in the texture analysis process used by Daginawala et al, and it is possible that employment of a filtration-histogram technique used here extracts and enhances subtle features/objects potentially improving the diagnostic capability.

There has been increasing interest in non-invasive imaging biomarkers of hepatic fibrosis, with particular attention to elastography (US, MR) techniques. For identifying significant fibrosis (≥F2), US elastography has reported ROC AUC values ranging from 0.840 to 0.870 [38] with sensitivity and specificity from 70-79% and 81-85% respectively. A meta-analysis looking at MR elastography for identifying significant

fibrosis showed AUC 0.880, sensitivity 79%, specificity 81%, similar to the US based results [7]. However, US is operator dependent and may be limited in obese or very ill patients, and with MRI failure rates may exceed 5% [12]. Both techniques must be performed prospectively with special equipment, and both are based on changes in stiffness, which is not specific to fibrosis. Increases in stiffness can also be seen in the setting of inflammation, which can overlap or coexist with hepatic fibrosis. CT based imaging biomarkers in general may be more easily and consistently applied, and may have the ability to differentiate inflammation vs fibrosis as they don't rely solely on changes in stiffness in the assessment, although this needs to be an area of future study. For example, in a study looking at lung cancer, the investigators were able to create regional histopathologic maps using CT features (HU histogram) to identify things like inactive fibrosis, active fibrosis, necrosis, red blood cells and neoplastic cells. In a liver that has a combination of processes such as inflammation and fibrosis, such maps may be useful in determining the predominant process, targeting biopsy, and prioritizing treatment [39].

A number of other promising CT based imaging parameters have been assessed. One is the liver segmental volume ratio (LSVR), which looks at the ratio of volume changes between segment I-III and segment IV-VIII[15]. As the degree of fibrosis increases, there is increasing hypertrophy of the left lateral segment and caudate lobe compared to the right lobe and medial left lobe, so the LSVR increases with increasing fibrosis. LSVR showed an ROC AUC value of 0.854 with sensitivity of 68% and specificity of 88% for identifying significant fibrosis (≥F2) using a threshold of 0.336 and of 0.880, 72%, and 88% respectively, for identifying advanced fibrosis (≥F3) using a threshold of 0.347. Similarly, changes in splenic volume were also found to correlate as well or better with stage of hepatic fibrosis, and when LSVR and splenic volume were taken together, improved ROC AUC values were seen. However, changes in total liver volume were not useful in predicting stage of fibrosis [15, 16]. This idea of differential changes in segments I-III vs IV-VIII is what compelled us in our study to measure these sections of liver separately in addition to the total hepatic texture. This may be why CT texture assessment of segment IV-VIII was the best predictor of stage of hepatic fibrosis, as segments I-III may be changing more slowly, or possibly in the opposite direction and measurements of the total liver become diluted as a result. This also supports the idea that measurements such as CTTA may be used for triaging for or even targeting of hepatic biopsy. Our practice frequently targets the left lobe for random biopsy, but these data suggest that that may underestimate the global amount of fibrosis in the liver. One potential drawback of the LSVR is that it may take a period of time and a certain amount of fibrosis for volume

changes to begin, so it was more difficult to separate earlier stages of fibrosis (F0, F1) using this technique. However, CTTA seems to capture some of the early changes happening within the parenchyma and multiple features, but particularly the mean gray level intensity at different filter scales (fine, medium, coarse), showed promise in differentiating no fibrosis (F0) from fibrosis (F1-F4), suggesting texture and volumetric measurements may be complementary.

Another CT imaging biomarker that has shown promising in assessing stage of hepatic fibrosis is liver surface nodularity (LSN), which is a simple objective measurement that quantifies the amount of surface nodularity along a section of liver [13]. For significant fibrosis, LSN showed an ROC AUC value of 0.902, for advanced fibrosis 0.932, and for cirrhosis, 0.959 [14]. This also showed promise in early stages of disease with an ROC AUC of 0.903 for F0 vs F1-F4 [14]. Like CTTA, the liver surface nodularity score is likely capturing changes that occur before substantial volumetric changes are seen.

Given that all three of these measures can be easily retrospectively obtained and may be complementary, multi-parametric assessment using all three may demonstrate improved performance and this is a goal of future work.

Limitations of this study include that texture analysis was only performed on a single slice of the liver rather than the entire volume of the liver. However, several studies have shown that use of a single slice is sufficient for sampling and extracting subtle features relevant for the clinical application being evaluated [22, 40]. In addition, the cohort was a pooled group of liver disease with a variety of etiologies included. Future work with larger, disease specific cohorts is planned. Although all the patients with intermediate stages of fibrosis underwent percutaneous biopsy, none of the patients in the normal cohort and some of the patients in the cirrhotic cohort did not have biopsy/tissue sampling. It is possible that some of our healthy controls may have had early unsuspected fibrosis, although the differentiation of F0 from F1-F4 seen consistently in this cohort might argue against that. For our F4 cohort, the decision not to require biopsy (although about half had a biopsy) was based on clinical practice of our hepatologists, who often don't order liver biopsy if the patient has an established

etiology for liver disease, imaging findings of cirrhosis, and clinical complications of cirrhosis/portal hypertension.

In conclusion, CT texture analysis of the liver parenchyma, particularly segments IV-VIII, may be a useful, non-invasive imaging biomarker for staging hepatic fibrosis that can easily be performed retrospectively or from routinely acquired CT and on serial CT examinations.

Table 1. Summary statistics for Mean, Skewness, Kurtosis at coarse filter (ssf 6)

		Average (SD)			**Median (range)**		
Texture Feature	**Fibrosis stage**	Seg IV-VIII	Total	Seg I-III	Seg IV-VIII	Total	Seg I-III
Mean	Pooled	0.92 (1.2)	1.94 (1.4)	5.09 (3.4)	0.66 (-0.9, 6.1)	1.84 (-0.9, 11.0)	4.56 (-3.0, 30.4)
	0	0.24 (0.6)	0.82 (0.8)	3.84 (2.4)	0.16 (-0.7, 1.9)	0.65 (-0.4, 4.1)	3.51 (-0.3, 14.4)
	1	0.76 (0.8)	1.95 (0.9)	6.36 (3.4)	0.6 (-0.6, 4.3)	1.79 (0.4, 4)	5.88 (1.8, 20.6)
	2	0.84 (1.1)	1.98 (1.1)	5.26 (2.7)	0.61 (-0.9, 3.6)	1.91 (0.2,4.0)	5.12 (1.0, 12.8)
	3	0.89 (0.9)	1.98 (1.2)	5.22 (3.5)	0.84 (-0.9, 3.9)	1.94 (-0.9, 5.6)	5.13 (-3.0, 17.7)
	4	1.74 (1.4)	3.00 (1.7)	5.48 (4.0)	1.56 (-0.8, 6.1)	2.65 (0.57, 11.0)	4.64 (0.3, 30.3)
Skewness	Pooled	1.65 (1.0)	1.46 (1.1)	-0.29 (1.5)	1.77 (-2.8, 4.1)	1.62 (-2.9, 3.5)	-0.04 (-5, 2.8)
	0	2.09 (0.6)	1.85 (0.8)	0.26 (1.2)	2.01 (1, 3.3)	1.89 (-2.3, 3.4)	0.32 (-2.7, 2.3)
	1	2.13 (0.7)	1.88 (0.8)	-0.19 (1.2)	2.15 (-0.3, 3.7)	1.9 (-0.2, 3.5)	-0.27 (-2.8, 2.8)
	2	2.10 (0.9)	1.89 (1.1)	0.34 (1.2)	2.14 (-0.3, 4.1)	2.1 (-2.2, 3.5)	0.51 (-2.3, 2.6)
	3	1.77 (1.1)	1.6 (1.1)	0.03 (1.3)	1.81 (-1.3, 3.4)	1.6 (-1.4, 3.2)	0.06 (-2.6, 2.8)
	4	0.68 (0.9)	0.6 (1.0)	-1.38 (1.7)	0.54 (-2.8, 3.1)	0.6 (-2.9, 2.7)	-1.21 (-5, 1.4)
Kurtosis	Pooled	8.22 (5.3)	8.60 (5.5)	7.64 (8.3)	7.66 (-0.1, 26.4)	8.06 (0.3, 32.6)	5.07 (-0.3, 55.6)
	0	8.95 (3.9)	8.91 (4.8)	5.42 (3.7)	8.50 (2.9, 18.9)	7.93 (2.9, 29.2)	4.62 (-0.3, 18.7)
	1	10.39 (4.5)	9.86 (4.4)	5.65 (4.9)	10.05 (2.8, 21.6)	9.21 (2.61, 23.0)	4.78 (0.1, 22.1)
	2	11.04 (6.2)	11.10 (4.8)	5.55 (4.2)	9.77 (1.8, 26.4)	10.60 (2.9, 21.1)	4.72 (0.1, 17.2)
	3	9.91 (5.5)	10.20 (6.2)	6.89 (6.5)	9.57 (0.3, 22.1)	9.19 (1.0, 32.6)	6.0 (0.1, 33.3)
	4	3.88 (3.6)	5.30 (4.9)	12.35 (12.7)	3.01 (-0.1, 17.4)	3.67 (0.3, 23.6)	7.7 (-0.2, 55.6)

Table 2

Texture parameter	Filter (SSF)	Comparison fibrosis stage	AUC	95% CI	p-value	Threshold	Sensitivity	Specificity
Mean	2	0 vs 1-4	**0.78**	0.72,0.84	<0.001	>0.175	0.74	0.74
Entropy	2	0 vs 1-4	0.74	0.67, 0.81	<0.001	>4.835	0.72	0.73
Mean	3	0 vs 1-4	0.77	0.72, 0.83	<0.001	>0.245	0.72	0.71
Mean	4	0 vs 1-4	0.77	0.71,0.82	<0.001	>0.295	0.73	0.7
Mean	5	0 vs 1-4	0.76	0.71, 0.82	<0.001	>0.365	0.71	0.69
Mean	5	0-1 vs 2-4	0.73	0.67, 0.78	<0.001	>0.425	0.7	0.63
Mean	6	0-2 vs 3-4	0.73	0.67, 0.79	<0.001	>0.605	0.7	0.62
Mean	6	0-3 vs 4	0.76	0.69, 0.82	<0.001	>0.94	0.7	0.7
Skewness	5	0-3 vs 4	**0.84**	0.79, 0.89	<0.001	<1.36	0.78	0.72
Skewness	6	0-3 vs 4	**0.87**	0.83, 0.92	<0.001	<1.29	0.84	0.75
Kurtosis	6	0-3 vs 4	**0.86**	0.81, 0.91	<0.001	<5.24	0.81	0.76

SSF=spatial scaling factor, AUC=Area under curve (**bold values represent highest AUCs**), CI=confidence interval

All measurements for this table were made in segments IV-VIII; threshold indicates for higher stages of fibrosis (example, Mean SSF 2, increases with increasing stage of fibrosis, Mean >0.175 likely represents stage 1-4 compared to F0)

Figures and Legends

Figure 1:

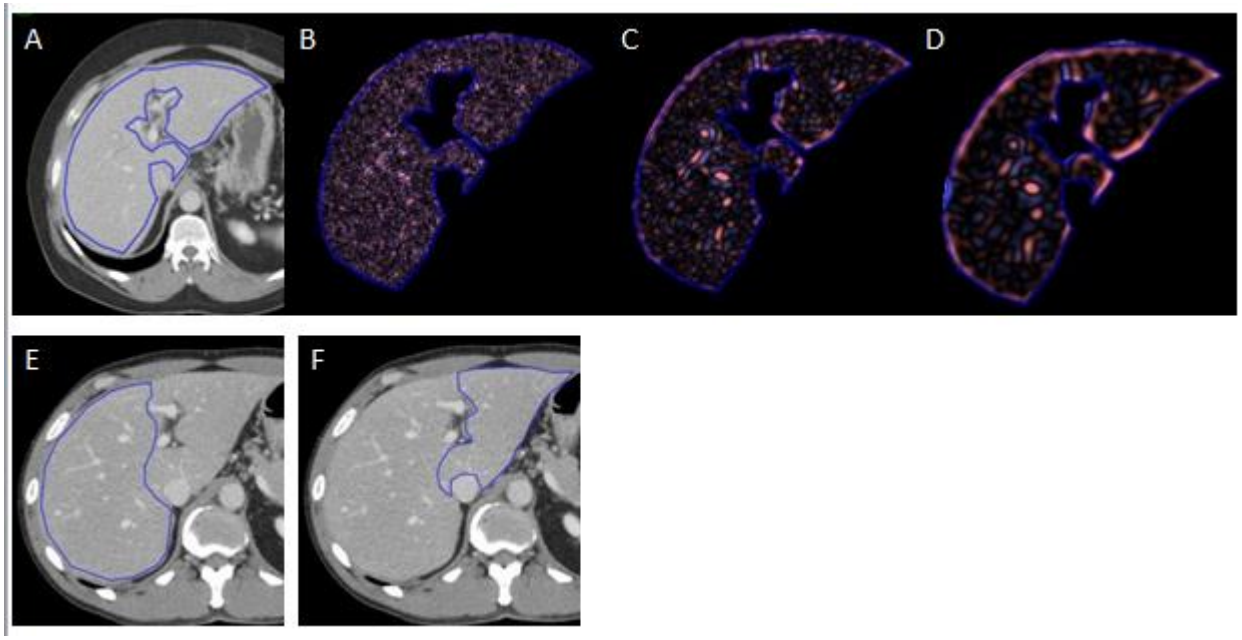

Figure 1: Texture measurements of the liver. Single slice CT image demonstrates an ROI drawn around the total liver at the level of the porta hepatis (A) in a pt with F3 disease. Fine (B), medium (C) and coarse filter (D) texture output is obtained. Similarly, ROIs were place on segments IV-VIII (E) and segments I-III (F) for additional analysis.

Figure 2:

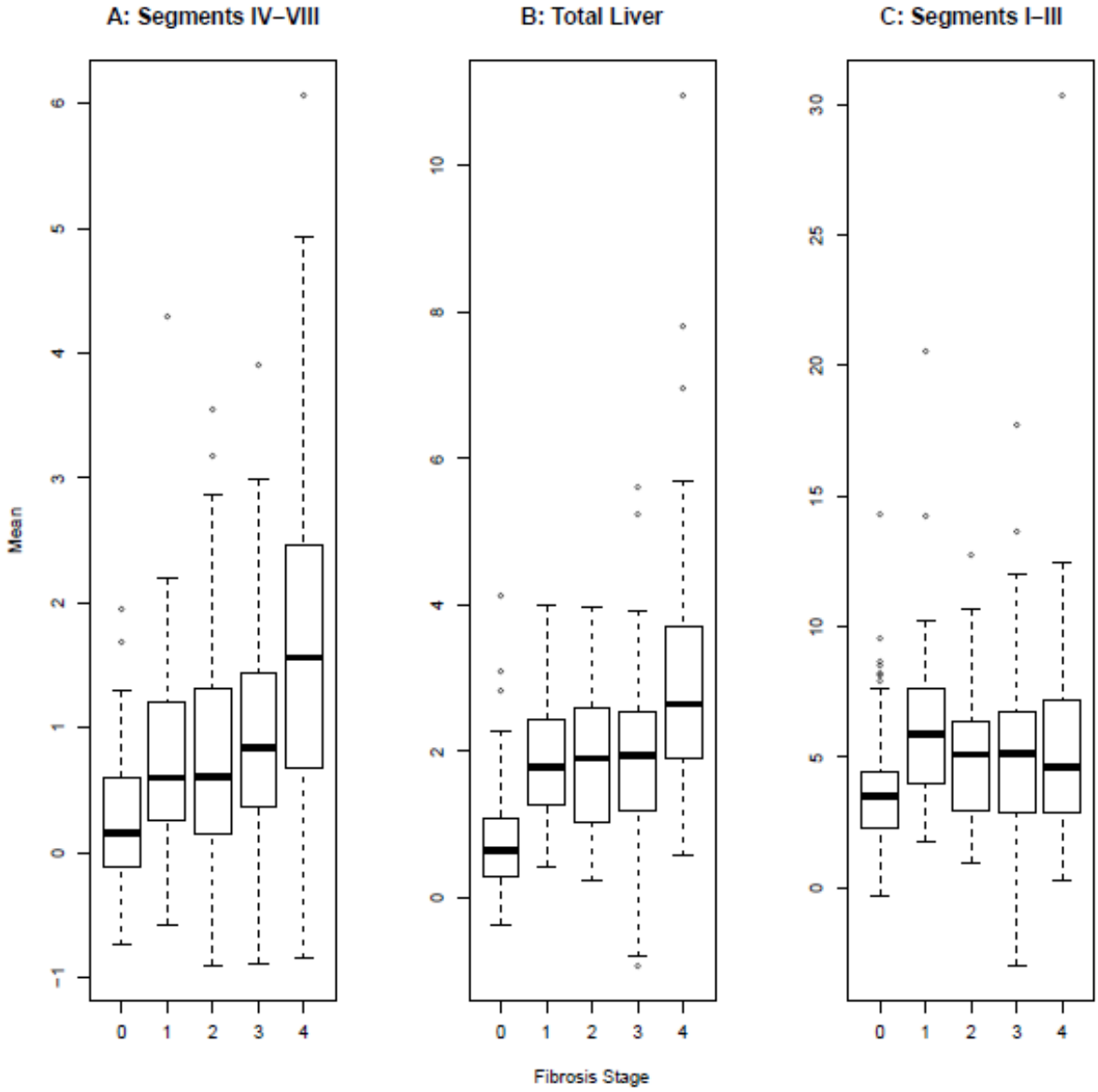

Figure 2: Boxplots for mean gray level intensity (y-axis) across fibrosis stages (x-axis, 0-4) at coarse feature size (SSF 6) for segments IV-VIII (A), total liver (B) and segments I-III (C). Note how the values increase across levels of fibrosis seen most prominently in segments IV-VIII, with a much less prominent or possibly opposite effect in segments I-III and a slightly diluted effect seen in the combined total liver.

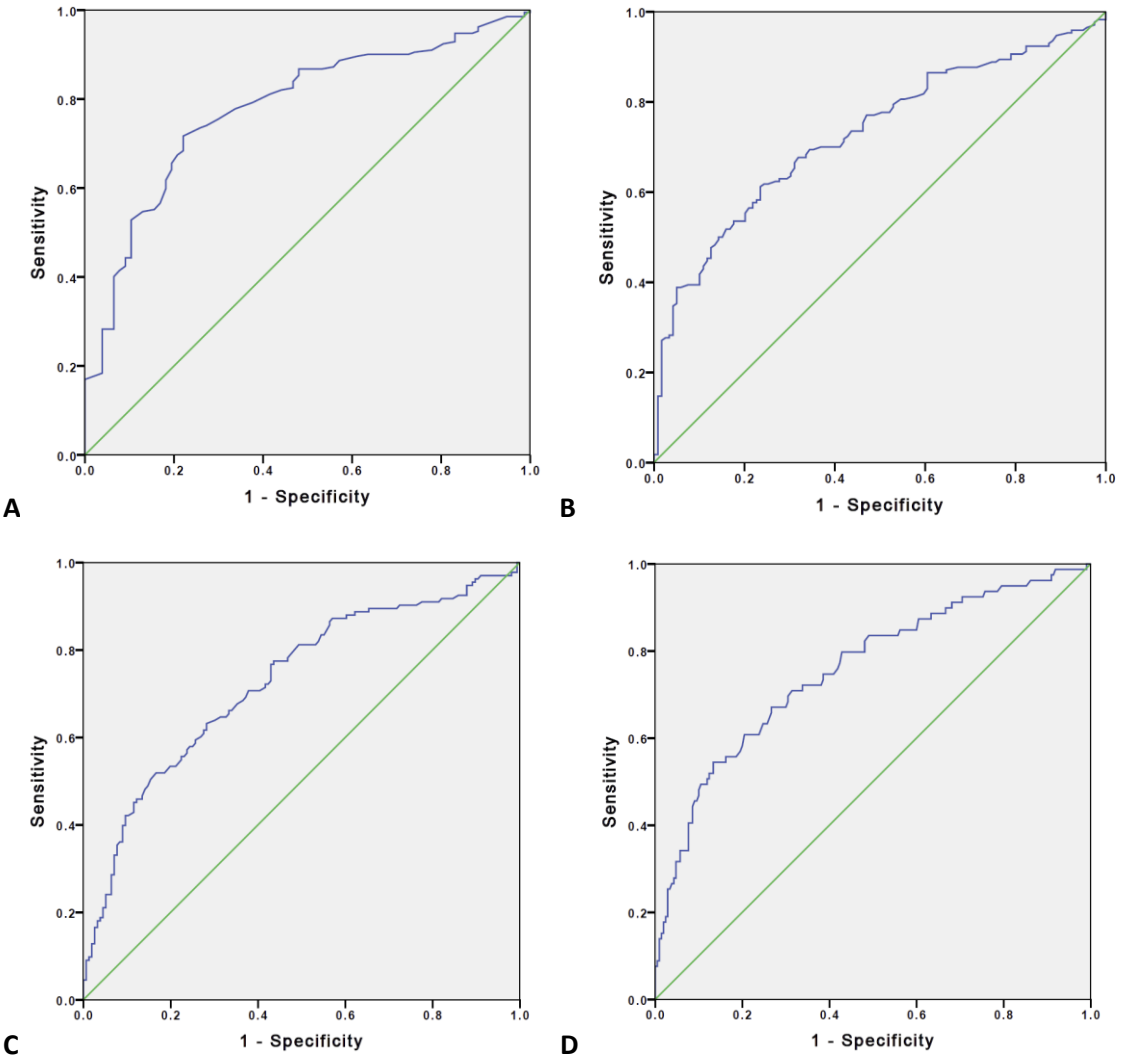

Figure 3: ROC analysis for mean gray level intensity (mean) compared to stage of fibrosis in segments IV-VIII. AUC for mean at fine feature size (SSF 2) for detecting presence of fibrosis (stage 0 vs 1-4, A) was 0.78, AUC for mean at medium feature size (SSF 5) for detecting significant fibrosis (≥F2, B) was 0.73, AUC for mean at coarse feature size (SSF 6) for detecting advanced fibrosis (≥F3, C) was 0.73, and AUC for mean at coarse feature size (SSF 6) for detecting cirrhosis (F4, D) was 0.76.

Figure 4:

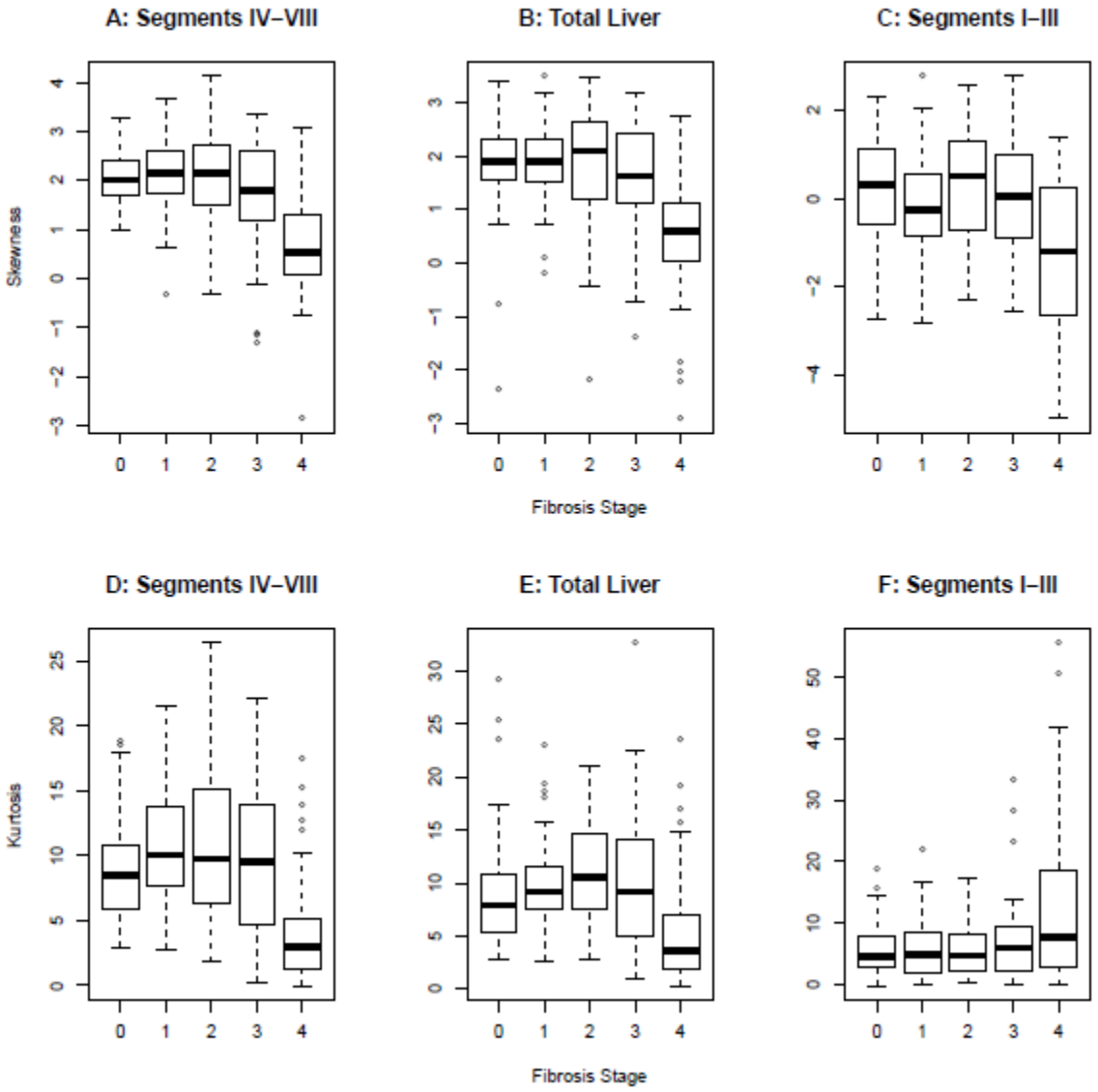

Figure 4: Boxplots for skewness (y-axis) at coarse feature size (SSF 6) comparing cirrhotics (F4) to other stages of fibrosis (F0-F3, x-axis) measured in segments IV-VIII (A), total liver (B) and segments I-III (C). There is a decrease in skewness values for F4 (cirrhosis) compared to F0-F3, seen most prominently is segments IV-VIIII. A similar trend is seen for kurtosis at coarse feature size (SSF 6) comparing F4 to other stages of fibrosis measured in segments IV-VIII (D), total liver (E), and segments I-III (F). In fact, kurtosis in F4 appears to have the opposite pattern relative to F0-F3 for segments IV-VIII versus sgments I-III.

Figure 5:

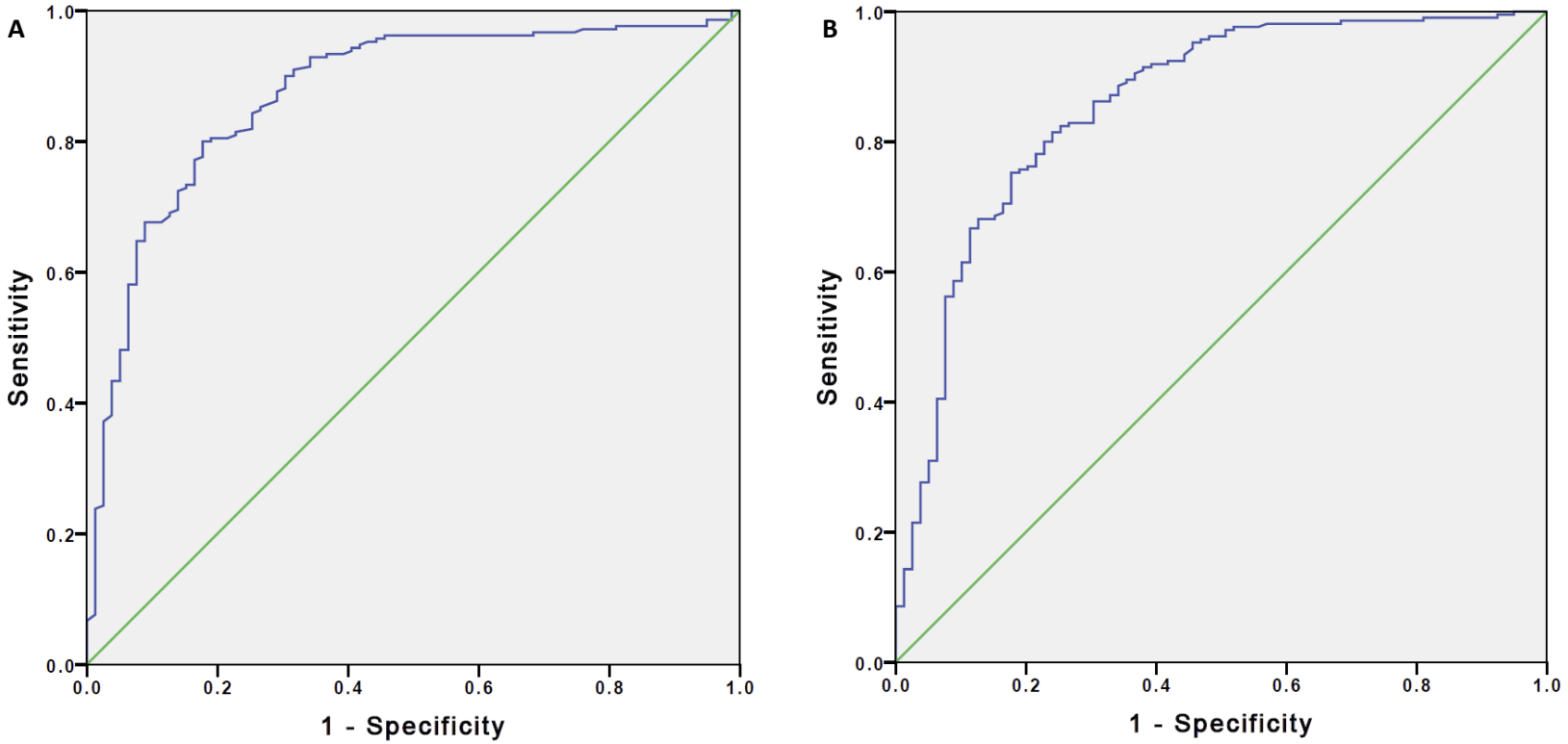

Figure 5: ROC analysis for skewness at coarse filter in segments IV-VIII for detecting cirrhosis (F4, A) with AUC of 0.87 and for kurtosis at coarse feature size (SSF 6) for cirrhosis (F4, B) with AUC of 0.86.

References:

1. Srinivasa Babu A, Wells ML, Teytelboym OM, et al. Elastography in Chronic Liver Disease: Modalities, Techniques, Limitations, and Future Directions. *Radiographics : a review publication of the Radiological Society of North America, Inc* 2016;
2. Prevention CfDCa. Viral Hepatitis. In: *Centers for Disease Control and Prevention Website*. www.cdc.gov/hepatitis/index.htm, Updated September 18, 2014
3. Afdhal NH, Nunes D. Evaluation of liver fibrosis: A concise review. *Am J Gastroenterol* 2004; 99:1160-1174
4. Martinez SM, Crespo G, Navasa M, Forns X. Noninvasive Assessment of Liver Fibrosis. *Hepatology* 2011; 53:325-335
5. Friedrich-Rust M, Nierhoff J, Lupsor M, et al. Performance of Acoustic Radiation Force Impulse imaging for the staging of liver fibrosis: a pooled meta-analysis. *Journal of Viral Hepatitis* 2012; 19:E212-E219
6. Friedrich-Rust M, Ong M-F, Martens S, et al. Performance of transient elastography for the staging of liver fibrosis: A meta-analysis. *Gastroenterology* 2008; 134:960-974
7. Singh S, Venkatesh SK, Wang Z, et al. Diagnostic Performance of Magnetic Resonance Elastography in Staging Liver Fibrosis: A Systematic Review and Meta-analysis of Individual Participant Data. *Clinical Gastroenterology and Hepatology* 2015; 13:440-451
8. Talwalkar JA, Kurtz DM, Schoenleber SJ, West CP, Montori VM. Utrasound-based transient elastography for the detection of hepatic fibrosis: Systematic review and meta-analysis. *Clinical Gastroenterology and Hepatology* 2007; 5:1214-1220
9. Wang Q-B, Zhu H, Liu H-L, Zhang B. Performance of magnetic resonance elastography and diffusion-weighted imaging for the staging of hepatic fibrosis: A meta-analysis. *Hepatology* 2012; 56:239-247
10. Castera L, Vergniol J, Foucher J, et al. Prospective comparison of transient elastography, fibrotest, APRI, and liver biopsy for the assessment of fibrosis in chronic hepatitis C. *Gastroenterology* 2005; 128:343-350
11. Foucher J, Chanteloup E, Vergniol J, et al. Diagnosis of cirrhosis by transient elastography (FibroScan): a prospective study. *Gut* 2006; 55:403-408
12. Yin M, Glaser KJ, Talwalkar JA, Chen J, Manduca A, Ehman RL. Hepatic MR Elastography: Clinical Performance in a Series of 1377 Consecutive Examinations. *Radiology* 2016; 278:114-124
13. Smith AD, Branch CR, Zand K, et al. Liver Surface Nodularity Quantification from Routine CT Images as a Biomarker for Detection and Evaluation of Cirrhosis. *Radiology* 2016; 280:771-781
14. Pickhardt PJ, Malecki K, Kloke J, Lubner MG. Accuracy of Liver Surface Nodularity Quantification on MDCT as a Noninvasive Biomarker for Staging Hepatic Fibrosis. *AJR American journal of roentgenology* 2016:1-6
15. Furusato Hunt OM, Lubner MG, Ziemlewicz TJ, Munoz Del Rio A, Pickhardt PJ. The Liver Segmental Volume Ratio for Noninvasive Detection of Cirrhosis: Comparison With Established Linear and Volumetric Measures. *Journal of computer assisted tomography* 2016; 40:478-484
16. Pickhardt PJ MK, Hunt OF, Beaumont C, Kloke J, Ziemlewicz TJ, Lubner MG. Hepatosplenic volumetric assessment at MDCT for staging liver fibrosis. *European radiology* 2016; Accepted
17. Ganeshan B, Miles KA. Quantifying tumour heterogeneity with CT. *Cancer imaging : the official publication of the International Cancer Imaging Society* 2013; 13:140-149
18. Davnall F, Yip CS, Ljungqvist G, et al. Assessment of tumor heterogeneity: an emerging imaging tool for clinical practice? *Insights Imaging* 2012; 3:573-589
19. Ganeshan B, Abaleke S, Young RC, Chatwin CR, Miles KA. Texture analysis of non-small cell lung cancer on unenhanced computed tomography: initial evidence for a relationship with tumour

glucose metabolism and stage. *Cancer imaging : the official publication of the International Cancer Imaging Society* 2010; 10:137-143
20. Ganeshan B, Goh V, Mandeville HC, Ng QS, Hoskin PJ, Miles KA. Non-small cell lung cancer: histopathologic correlates for texture parameters at CT. *Radiology* 2013; 266:326-336
21. Ganeshan B, Panayiotou E, Burnand K, Dizdarevic S, Miles K. Tumour heterogeneity in non-small cell lung carcinoma assessed by CT texture analysis: a potential marker of survival. *European radiology* 2012; 22:796-802
22. Lubner MG, Stabo N, Lubner SJ, et al. CT textural analysis of hepatic metastatic colorectal cancer: pre-treatment tumor heterogeneity correlates with pathology and clinical outcomes. *Abdominal imaging* 2015;
23. Ng F, Ganeshan B, Kozarski R, Miles KA, Goh V. Assessment of primary colorectal cancer heterogeneity by using whole-tumor texture analysis: contrast-enhanced CT texture as a biomarker of 5-year survival. *Radiology* 2013; 266:177-184
24. Smith AD, Gray MR, Del Campo SM, et al. Predicting Overall Survival in Patients With Metastatic Melanoma on Antiangiogenic Therapy and RECIST Stable Disease on Initial Posttherapy Images Using CT Texture Analysis. *AJR American journal of roentgenology* 2015; 205:W283-293
25. Stabo N LM, Abel EJ, Munoz del Rio A, Pickhardt PJ. CT textural analysis of large primary renal cell carcinomas: Tumor heterogeneity correlates with histology and clinical outcomes. In: *Society of Abdominal Radiology*. San Diego, CA, 2014
26. Raman SP, Chen Y, Schroeder JL, Huang P, Fishman EK. CT Texture Analysis of Renal Masses: Pilot Study Using Random Forest Classification for Prediction of Pathology. *Academic radiology* 2014; 21:1587-1596
27. Weiss GJ, Ganeshan B, Miles KA, et al. Noninvasive Image Texture Analysis Differentiates K-ras Mutation from Pan-Wildtype NSCLC and Is Prognostic. *PloS one* 2014; 9:e100244
28. Yip C, Landau D, Kozarski R, et al. Primary esophageal cancer: heterogeneity as potential prognostic biomarker in patients treated with definitive chemotherapy and radiation therapy. *Radiology* 2014; 270:141-148
29. Fujita A, Buch K, Li B, Kawashima Y, Qureshi MM, Sakai O. Difference Between HPV-Positive and HPV-Negative Non-Oropharyngeal Head and Neck Cancer: Texture Analysis Features on CT. *Journal of computer assisted tomography* 2016; 40:43-47
30. Goh V, Ganeshan B, Nathan P, Juttla JK, Vinayan A, Miles KA. Assessment of response to tyrosine kinase inhibitors in metastatic renal cell cancer: CT texture as a predictive biomarker. *Radiology* 2011; 261:165-171
31. Ozkan E, West A, Dedelow JA, et al. CT Gray-Level Texture Analysis as a Quantitative Imaging Biomarker of Epidermal Growth Factor Receptor Mutation Status in Adenocarcinoma of the Lung. *AJR American journal of roentgenology* 2015; 205:1016-1025
32. Ginsburg SB, Zhao J, Humphries S, et al. Texture-based Quantification of Centrilobular Emphysema and Centrilobular Nodularity in Longitudinal CT Scans of Current and Former Smokers. *Academic radiology* 2016;
33. Park HJ, Lee SM, Song JW, et al. Texture-Based Automated Quantitative Assessment of Regional Patterns on Initial CT in Patients With Idiopathic Pulmonary Fibrosis: Relationship to Decline in Forced Vital Capacity. *AJR American journal of roentgenology* 2016:1-8
34. Daginawala N, Li B, Buch K, et al. Using texture analyses of contrast enhanced CT to assess hepatic fibrosis. *European journal of radiology* 2016; 85:511-517
35. Bedossa P, Poynard T. An algorithm for the grading of activity in chronic hepatitis C. The METAVIR Cooperative Study Group. *Hepatology* 1996; 24:289-293

36. Miles KA, Ganeshan B, Hayball MP. CT texture analysis using the filtration-histogram method: what do the measurements mean? *Cancer imaging : the official publication of the International Cancer Imaging Society* 2013; 13:400-406
37. Ganeshan B, Miles KA, Young RC, Chatwin CR. Texture analysis in non-contrast enhanced CT: impact of malignancy on texture in apparently disease-free areas of the liver. *European journal of radiology* 2009; 70:101-110
38. Tang A, Cloutier G, Szeverenyi NM, Sirlin CB. Ultrasound Elastography and MR Elastography for Assessing Liver Fibrosis: Part 2, Diagnostic Performance, Confounders, and Future Directions. *American Journal of Roentgenology* 2015; 205:33-40
39. Sieren JC, Smith AR, Thiesse J, et al. Exploration of the volumetric composition of human lung cancer nodules in correlated histopathology and computed tomography. *Lung cancer (Amsterdam, Netherlands)* 2011; 74:61-68
40. Ng F, Kozarski R, Ganeshan B, Goh V. Assessment of tumor heterogeneity by CT texture analysis: can the largest cross-sectional area be used as an alternative to whole tumor analysis? *European journal of radiology* 2013; 82:342-348